NASA

DEPARTMENT OF MECHANICAL ENGINEERING AND MECHANICS
SCHOOL OF ENGINEERING
OLD DOMINION UNIVERSITY
NORFOLK, VIRGINIA 23508

RESPONSE TIME FOR MULTILAYERED PLATINUM RESISTANCE THERMOMETERS

By

D. K. Pandey, Co-Principal Investigator

and

R. L. Ash, Principal Investigator

Final Report
For the period December 4, 1984 to March 30, 1985

Prepared for
National Aeronautics and Space Administration
Langley Research Center
Hampton, Virginia 23665

Under
Master Contract Agreement NAS-1-17099
Task Authorization No. 43
L.A. Dillon-Townes, Technical Monitor
IRD-Thermal Instrumentation Section

(NASA-CR-176655) RESPONSE TIME FOR MULTILAYERED PLATINUM RESISTANCE THERMOMETERS Final Report, 4 Dec. 1984 - 30 Mar. 1985 (Old Dominion Univ.) 34 p HC A03/MF A01 CSCL 14B G3/35
N86-21816
Unclas
15845

July 1985

DEPARTMENT OF MECHANICAL ENGINEERING & MECHANICS
SCHOOL OF ENGINEERING
OLD DOMINION UNIVERSITY
NORFOLK, VIRGINIA 23508

RESPONSE TIME FOR MULTILAYERED PLATINUM RESISTANCE THERMOMETERS

By

D. K. Pandey, Co-Principal Investigator

and

R. L. Ash, Principal Investigator

Final Report
For the period December 4, 1984 to March 30, 1985

Prepared for
National Aeronautics and Space Administration
Langley Research Center
Hampton, Virginia 23665

Under
Master Contract Agreement NAS-1-17099
Task Authorization No. 43
L.A. Dillon-Townes, Technical Monitor
IRD-Thermal Instrumentation Section

Submitted by the
Old Dominion University Research Foundation
P.O. Box 6369
Norfolk, Virginia 23508

July 1985

FOREWORD

This work was supported by the NASA Langley Research Center under the Master Contract Agreement NAS-1-17099, Task Authorization 43, and monitored by Mr. L. A. Dillon-Townes of the IRD-Thermal Instrumentation Section, NASA Langley Research Center, Mail Stop 234, Hampton, VA 23665.

SUMMARY

Response time constants for several multilayered temperature transducers were determined numerically by using Martin Marietta's MITAS software package which is available at NASA Langley Research Center. Present results were found in close agreement with the solutions reported in the literature, thus, the capability of MITAS was justified. On the basis of experiences gained, the MITAS is recommended for use in predicting the response time constants of sensors by an in-situ technique.

TABLE OF CONTENTS

LIST OF TABLES

TABLE OF CONTENTS - continued

LIST OF TABLES - continued

LIST OF FIGURES

RESPONSE TIME FOR MULTILAYERED PLATINUM RESISTANCE THERMOMETERS

By

D. K. Pandey[1], Co-Principal Investigator
R. L. Ash[2], Principal Investigator

1. INTRODUCTION

Response time correlations for two platinum resistance thermometers (PRT's), the HyCal (100 ohm) and the Rosemount (1000 ohm), were established by Pandey et al. (Refs. 1, 2). These correlations can predict the time constants within 5% of experimental results. One of the PRT's, the Rosemount (1000 ohm) Sensor, is found to be more accurate and suitable for use in cryogenic environments. The objective, therefore, was to model this multilayered sensor to predict its response behavior under different conditions, theoretically.

Lowell and Patton (Ref. 3) predicted the response behavior of homogeneous laminated cylinders exposed to sinusoidal temperature variation. Their work is applicable to hot wire anemometry and thermocouple pyrometry. Bulavin and Kashcheev (Ref. 4) solved the non-homogeneous heat conduction equation for multilayered bodies by the method of separated variables. Further, Mulholland (Ref. 5) applied the Fourier transform to laminated orthotropic cylinders, and then used a unique orthogonality relationship.

The most relevant literature for the present work is Kerlin et al. (Ref. 6) who have solved the multilayered cylindrical problems, numerically. It was proposed, however, to use the Martin Marietta Thermal Analysis

---

[1] Research Assistant Professor, Department of Mechanical Engineering and Mechanics, Old Dominion University, Norfolk, Virginia 23508.

[2] Chairman, Department of Mechanical Engineering, Old Dominion University, Norfolk, Virginia 23508.

computer package (MITAS) to obtain the response time constants of the multi-layered PRT's under different environmental conditions.

2. DESCRIPTION OF THE SENSOR

The Rosemount Sensor shown in Figure 1 was considered for mathematical modeling. This sensor had a 1000 ohm reference resistance with sheath diameter, D_{sh} = 0.884. This sensor was dissected to determine the internal dimensions of the materials used by the manufacturer. The internal dimensions displayed in Figure 2 were determined using the best facility available at NASA/Langley Research Center. The mandrel is made of pure platinum, while the perforated sheath material is stainless steel. The ceramic used in the construction of this sensor was not specified, but to our best knowledge Aluminum oxide (Al_2O_3) was used and is assumed in this study. Thermophysical properties of these materials are given in Appendix A.

3. PHYSICAL MODEL

Modeling of the Rosemount Sensor, which considers the Rosemount's unique geometry as detailed in Figure 2, involves multi-dimensional flow and thermal phenomena into flowing fluids. Such complex geometry has never been attempted by the researchers and, in this short task project, it was necessary to reduce this complicated problem to a one dimensional problem. The perforated sheath, which enhances heat transfer, was dropped from further analysis by employing the results of Daryabeigi et al. (Ref. 8). The shroud effect on convection was included (but not the shroud mass). The physical model analyzed in this study is illustrated in Figure 3.

4. GOVERNING EQUATION

Heat transfer by conduction in a homogeneous hollow cylinder can be expressed as:

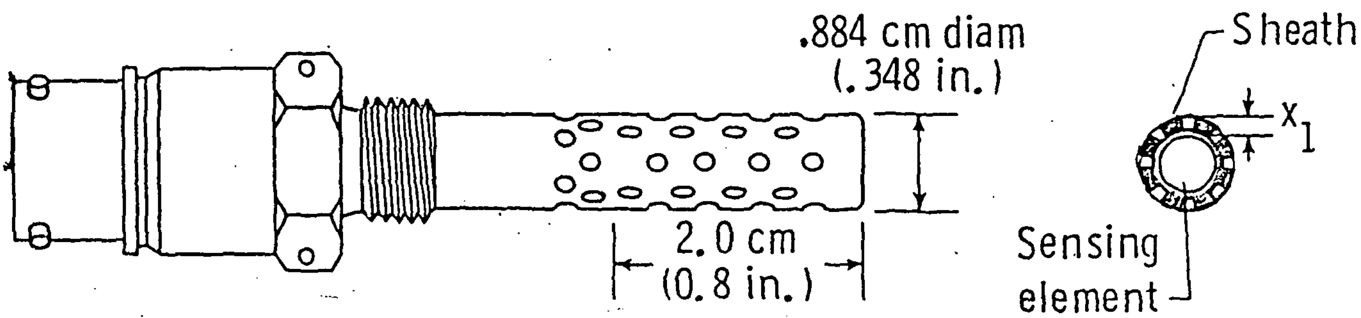

Figure 1. Rosemount Sensor (1000 ohm).

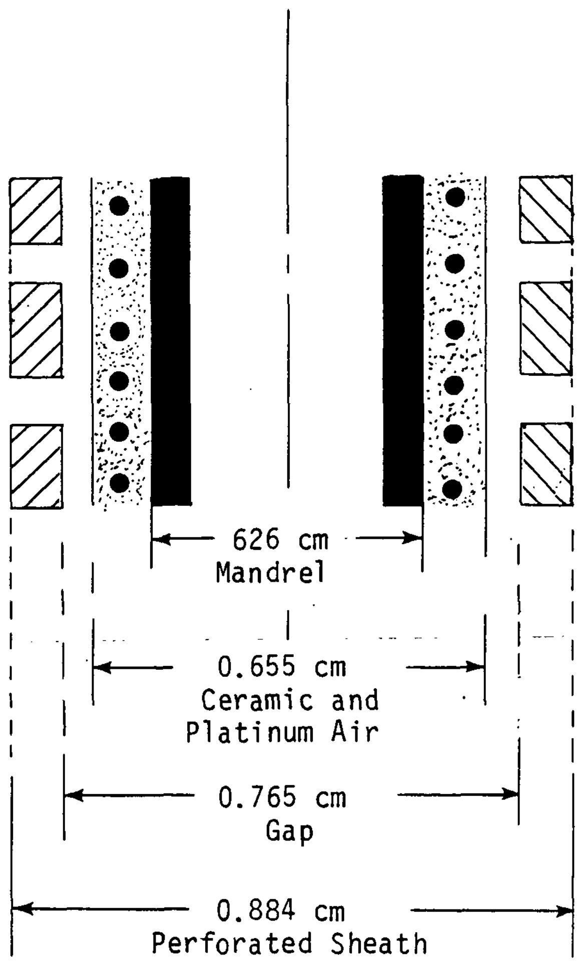

● Diameter of the platinum wire = 18×10^{-4} cm.

Figure 2. Internal Dimensions of the Rosemount Sensor.

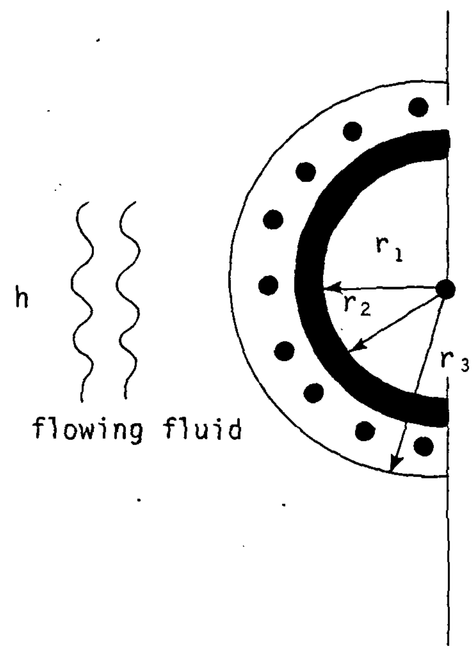

r_1: inner radius of mandrel

r_2: outer radius of mandrel

r_3: outer radius of matrix ($P_t + Al_2O_3$)

h: heat transfer coefficient between flowing fluid and the sensor

Figure 3. Physical Model.

$$\rho C_p \frac{\partial T}{\partial t} = k\nabla^2 \ T + \frac{\dot{Q}}{\rho C_p}$$

The above equation without heat generation ($\dot{Q}$) in a radial direction reduces to:

$$\rho C_p \frac{\partial T}{\partial t} = \frac{k}{r} \ \frac{\partial}{\partial r} (r \ \frac{\partial T}{\partial r}), \qquad r_2 > r > r_1 \quad . \tag{1}$$

The boundary and initial conditions are:

$$- k \frac{\partial T}{\partial r}\Bigg|_{r \ = \ r_2} = h \ (T- \ T_f) \tag{2}$$

$$\frac{\partial T}{\partial r}\Bigg|_{r \ = \ r_1} = 0 \tag{3}$$

$$T = T_i = \text{constant}, \quad r_2 > r > r_1, \ t = 0 \tag{4}$$

$$T = T_f = \text{constant}, \quad r > r_3, \ t = 0 \tag{5}$$

where

T	=	$T\ (r,\ t)$
t	=	time
r	=	radial position
k	=	thermal conductivity
h	=	heat transfer coefficient between fluid and surface
T_f	=	fluid temperature
T_i	=	Initial temperature.

Those equations can be solved exactly by using Laplace transforms and approximately by using a finite difference scheme. In this work, the lumped parametric method is employed to solve these equations.

5. LUMPED PARAMETER ANALYSIS

The nodal approach using a one-dimensional node to node heat transfer model, as illustrated in Figure 4, can be used for multilayered platinum resistance thermometers. The solution to any desired accuracy can be obtained by using many nodes. The governing equation (1) under lumped parametric analysis can be written as

$$(\rho C_p)_i \frac{dT_i}{dt} = C_i \ (T_{i+1} - T_i) + C_{i-1} \ (T_{i-1} - T_i) \tag{6}$$

where

$(\rho C_p)_i$ = heat capacity of the material at node i

T_i = Temperature at node i

C_i, C_{i-1} = heat transfer conductances between nodes.

6. SOLUTION PROCEDURE

The MITAS thermal analysis package (Ref. 7) is designed primarily to solve, lumped parameter, i.e., resistor-capacitor (R-C), network representations of thermal systems. This package is available at NASA/Langley Research Center and was used to solve equation (6). Instructions on how to use this package are described in Appendix B.

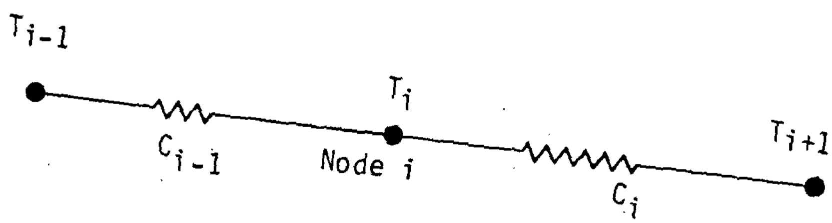

Figure 4. One Dimensional Heat Transfer Model.

7. VERIFICATION OF PRESENT SOLUTION PROCEDURE

To establish the applicability of the MITAS software package for solving the thermal problems; some cases of Kerlin et al. Ref. 6 were examined. Kerlin et al. (Ref. 6) have reported the time constants for multilayered hollow cylinders exposed to different convective boundaries.

8. KERLIN EXAMPLE FOR HOLLOW CYLINDER OF A SINGLE MATERIAL

Table 2 details the geometrical and thermal parameters for the hollow cylinders used in determining the time constant.

The hollow cylinder was divided into 9 equal regions. As required by the MITAS package, the conductances for every region were computed by using the equations detailed in Appendix B. The complete data for thermal conductances and capacitances used by the MITAS package are given in Appendix C. Table 3 displays variation in the dimensionless temperature at each node with time. The temperature at node 1 rises to its 63.2% level in 0.251 seconds. Therefore, the time constant for this problem is 0.251 seconds. The time constant for the same problem reported by Kerlin Ref. 6 is 0.257.

9. KERLIN EXAMPLE OF MULTILAYERED HOLLOW CYLINDER

Table 4 describes the problem solved by the MITAS software package to obtain the time constant. The temperature variation with time is given in Table 5. By interpolation, the time constant for this case at Node 1 is found to be 0.184 while Kerlin et al. (Ref. 6) have reported 0.181 seconds. In conclusion, the present results obtained by using the MITAS scheme are found in close agreement with Kerlin's (Ref. 6) solution. Thus the present solution procedure is justified and, therefore, it is extended to solve the present multilayered platinum resistance thermometers.

Table 2. Analysis Parameters for Hollow Cylinder

Outer radius $b = 47.625 \times 10^{-4}$ m

Inner radius $a = 42.544 \times 10^{-4}$ m

Density of the material $\rho = 7848.82 \ \frac{kg}{m^3}$

Thermal conductivity, k, $= 20.94 \ \frac{W}{m \ ^oC}$

Specific heat, $C_p = 502.43 \ \frac{W.Sec}{kg \ ^oC}$

Corrective heat transfer coefficient, $h = 7950 \ \frac{W}{m^2 \ ^oC}$

Number of regions for numerical case = 9.

Table 3. Dimensionless temperature (θ) history obtained by MITAS for example given in Table 2.

θ / t (second)	Node 1	Node 2	Node 3	Node 4	Node 5	Node 6	Node 7	Node 8	Node 9
0.0000	0.0000	0.0000	0.0000	0.0000	0.0000	0.0000	0.0000	0.0000	0.0000
.0180	.0470	.0486	.0519	.0569	.0638	.0727	.0838	.0976	.1143
.0360	.1259	.1270	.1291	.1321	.1356	.1393	.1428	.1455	.1465
.0540	.1820	.1829	.1846	.1874	.1913	.1968	.2043	.2145	.2284
.0720	.2416	.2428	.2452	.2485	.2527	.2572	.2616	.2650	.2661
.0900	.2948	.2954	.2967	.2987	.3015	.3055	.3111	.3192	.3311
.1080	.3437	.3448	.3469	.3500	.3539	.3583	.3626	.3661	.3671
.1260	.3910	.3916	.3927	.3944	.3967	.3998	.4043	.4108	.4212
.1440	.4327	.4336	.4354	.4380	.4414	.4454	.4495	.4528	.4535
.1620	.4738	.4743	.4754	.4769	.4789	.4815	.4850	.4905	.4995
.1800	.5098	.5105	.5120	.5142	.5171	.5206	.5244	.5274	.5280
.1980	.5452	.5457	.5467	.5481	.5499	.5520	.5549	.5594	.5674
.2160	.5765	.5771	.5782	.5800	.5825	.5856	.5890	.5918	.5921
.2340	.6069	.6074	.6083	.6096	.6111	.6130	.6154	.6191	.6261
.2520	.6341	.6346	.6355	.6370	.6391	.6418	.6449	.6475	.6476
.2700	.6602	.6607	.6615	.6627	.6641	.6656	.6676	.6707	.6769
.2880	.6839	.6842	.6850	.6862	.6880	.6904	.6931	.6955	.6954
.3060	.7063	.7067	.7075	.7085	.7098	.7111	.7127	.7153	.7208
.3240	.7268	.7271	.7278	.7288	.7303	.7323	.7348	.7370	.7367
.3420	.7461	.7465	.7472	.7482	.7493	.7504	.7517	.7538	.7588
.3600	.7640	.7642	.7647	.7656	.7669	.7686	.7708	.7728	.7725

Table 4. Parameters for Multilayered Hollow Cylinders

Number of regions = 3

Number of layers per region = 1, 4, 4

Material in region = platinum, aluminum oxide, stainless steel

Radii = 40.538×10^{-4}, 40.834×10^{-4}, 44.196×10^{-4}, 47.549×10^{-4} m

Convective heat transfer coefficient = 17036 $w/m^2\ ^oC$

Thermophysical properties are given in Appendix A.

Table 5. Dimensionless temperature (θ) history obtained by MITAS for example given in Table 4.

θ / t (second)	Node 1	Node 2	Node 3	Node 4	Node 5	Node 6	Node 7	Node 8	Node 9
0.0000	0.0000	0.0000	0.0000	0.0000	0.0000	0.0000	0.0000	0.0000	0.0000
.0180	.0403	.0446	.0525	.0629	.0763	.1084	.1294	.1574	.1936
.0360	.1626	.1637	.1687	.1768	.1871	.2095	.2195	.2271	.2297
.0540	.2438	.2470	.2518	.2576	.2649	.2825	.2952	.3141	.3423
.0720	.3232	.3245	.3290	.3363	.3458	.3668	.3768	.3849	.3871
.0900	.3871	.3908	.3960	.4017	.4080	.4223	.4318	.4460	.4689
.1080	.4487	.4497	.4535	.4596	.4677	.4861	.4953	.5030	.5047
.1260	.5011	.5045	.5093	.5141	.5192	.5303	.5373	.5480	.5667
.1440	.5515	.5522	.5549	.5600	.5665	.5814	.5893	.5962	.5972
.1620	.5915	.5944	.5986	.6027	.6074	.6175	.6232	.6314	.6472
.1800	.6257	.6272	.6306	.6356	.6415	.6545	.6616	.6681	.6689
.1980	.6569	.6597	.6636	.6674	.6717	.6808	.6855	.6920	.7055
.2160	.6899	.6902	.6922	.6958	.7003	.7106	.7166	.7224	.7228
.2340	.7061	.7101	.7148	.7191	.7235	.7322	.7363	.7415	.7530
.2520	.7379	.7375	.7388	.7418	.7455	.7543	.7597	.7651	.7654
.2700	.7488	.7529	.7572	.7609	.7646	.7718	.7750	.7791	.7890
.2880	.7691	.7692	.7713	.7748	.7788	.7877	.7928	.7980	.7982

10. RESPONSE OF ROSEMOUNT SENSOR IN FLOWING AIR

The internal dimensions of this sensor are given in Figure 2. The physical model used in this analysis is shown in Figure 3. The region of aluminum oxide, Al_2O_3 (a ceramic material) was divided into two layers and the sensing element -- platinum wire -- was taken as a single node. Thermal conductance and capacitance for each node computed for the MITAS package are given in Appendix D. The capacitance of the sensing element was computed by using the formula:

$$C_{10} = (\rho Cp)_{pt} \frac{1}{4} \Pi^2 (r_2 + r_1) (r_2 - r_1)^2.$$

The value of the boundary conductor (3099) is varied to see the effect on temperature histories in flowing air. Tables 6, 7 and 8 display the temperature histories for the Rosemount Sensor for boundary conductors (3099) 4.0, 6.0 and 8.0, respectively. One can note from tables 6 and 7 that temperatures increase rapidly then fluctuate and do not reach an identifiable 63.2% value. By increasing the convective heat transfer coefficient (boundary node), the temperature rises beyond 63.2% of total step change in temperature, but fluctuates about. Authors have tried to handle this problem by averaging the material properties, increasing the number of nodes and using the backward, forward and forward-backward techniques. Theoretical response time constants are not found comparable with the experimental time constant for the Rosemount Sensor in flowing air reported in Ref. 1. Thus, the uncertainties are due to the internal dimension of the sensor, properties of the ceramic material, convective heat transfer coefficient and multi-dimensional nature of heat transfer and fluid flow phenomenon.

Table 6. Dimensionless Temperature (θ) History of Rosemount Sensor (Boundary Conductance = 4.0).

θ t (second)	Node 1	Node 2	Node 3
0.0000	0.0000	0.0000	0.0000
1.0000	.0534	.0533	.0533
2.0000	.1038	.1038	.1038
3.0000	.1516	.1515	.1516
4.0000	.1968	.1968	.1968
5.0000	.2397	.2396	.2397
6.0000	.2460	.2461	.2461
7.0000	.2474	.2473	.2474
8.0000	.2477	.2479	.2479
9.0000	.2488	.2487	.2488
10.0000	.2490	.2491	.2491
11.0000	.2499	.2498	.2499
12.0000	.2501	.2498	.2502
13.0000	.2509	.2508	.2508
14.0000	.2509	.2510	.2510
15.0000	.2516	.2515	.2516
16.0000	.2516	.2518	.2518
17.0000	.2524	.2523	.2524
18.0000	.2524	.2526	.2526
19.0000	.2532	.2531	.2532
20.0000	.2532	.2533	.2540
21.0000	.2540	.2539	.2540
22.0000	.2540	.2541	.2541
23.0000	.2546	.2545	.2546
24.0000	.2546	.2547	.2547
25.0000	.2552	.2551	.2552
26.0000	.2552	.2554	.2554
27.0000	.2558	.2558	.2558
28.0000	.2559	.2560	.2560
29.0000	.2565	.2564	.2565
30.0000	.2565	.2566	.2566
31.0000	.2571	.2570	.2571
32.0000	.2571	.2572	.2572
33.0000	.2577	.2576	.2577

Table 7. Dimensionless Temperature (θ) History of Rosemount Sensor (Boundary Conductance = 6.0)

θ / t (second)	Node 1	Node 2	Node 3
0.0000	0.0000	0.0000	0.0000
1.0000	.0795	.0793	.0795
2.0000	.1526	.1526	.1526
3.0000	.2199	.2198	.2199
4.0000	.2818	.2819	.2818
5.0000	.3389	.3388	.3389
6.0000	.3914	.3914	.3914
7.0000	.4398	.4397	.4398
8.0000	.4842	.4843	.4842
9.0000	.4993	.4993	.4994
10.0000	.5001	.5002	.5001
11.0000	.5002	.5002	.5003
12.0000	.5010	.5011	.5010
13.0000	.5011	.5011	.5012
14.0000	.5018	.5018	.5018
15.0000	.5019	.5019	.5020
16.0000	.5026	.5026	.5026
17.0000	.5026	.5026	.5027
18.0000	.5033	.5034	.5033
19.0000	.5034	.5034	.5035
20.0000	.5041	.5041	.5041
21.0000	.5041	.5042	.5043
22.0000	.5047	.5047	.5047
23.0000	.5048	.5048	.5049
24.0000	.5053	.5053	.5053
25.0000	.5054	.5054	.5055
26.0000	.5059	.5060	.5059
27.0000	.5060	.5060	.5061
28.0000	.5065	.5066	.5065
29.0000	.5066	.5066	.5067
30.0000	.5071	.5072	.5071

Table 8. Dimensionless Temperature (θ) History of Rosemount Sensor (Boundary Conductance = 8.0).

θ / t (second)	Node 1	Node 2	Node 3
0.0000	0.0000	0.0000	0.0000
1.0000	.1053	.1051	.1053
2.0000	.1993	.1993	.1993
3.0000	.2836	.2834	.2836
4.0000	.3589	.3589	.3589
5.0000	.4264	.4262	.4264
6.0000	.4867	.4867	.4867
7.0000	.5408	.5406	.5407
8.0000	.5890	.5891	.5890
9.0000	.6320	.6320	.6321
10.0000	.6325	.6326	.6325
11.0000	.6326	.6326	.6327
12.0000	.6331	.6332	.6331
13.0000	.6332	.6332	.6333
14.0000	.6336	.6337	.6336
15.0000	.6337	.6337	.6338
16.0000	.6341	.6341	.6341
17.0000	.6341	.6341	.6343
18.0000	.6345	.6346	.6345
19.0000	.6346	.6346	.6347
20.0000	.6350	.6351	.6350
21.0000	.6351	.6351	.6352
22.0000	.6355	.6355	.6355
23.0000	.6355	.6355	.6357
24.0000	.6359	.6360	.6359
25.0000	.6360	.6360	.6361
26.0000	.6361	.6362	.6361
27.0000	.6362	.6362	.6363
28.0000	.6363	.6363	.6363
29.0000	.6363	.6363	.6364
30.0000	.6364	.6365	.6364

11. CONCLUSIONS AND RECOMMENDATIONS

1. The MITAS software package available at NASA Langley is found capable of predicting the response time constants of multilayered temperature transducers in flowing fluids.
2. The MITAS software package can also be used to predict the response time constants by In-situ technique.
3. The multilayered Rosemount sensor, which is unique in its internal structure, needs to be treated like multi-dimensional conduction problem. Note that such geometry has not yet been attempted by the researchers. Therefore, such analyses are needed to know exactly the response behavior of these sensors.
4. It is recommended that the in-site technique be analyzed theoretically and experimentally.

REFERENCES

1. Pandey, D.K., and R.L. Ash, "Response Time Correlation for Platinum Resistance Thermometers in Flowing Fluids," NASA Contractor Report CR-172523, 1985.

2. Pandey, D.K., L.A. Dillon-Townes, "Response Time Correlations for Platinum Resistance Thermometers," Proceedings of the 31st International Instrumentation Symposium," San Diego, CA, ISA, Research Triangle N.C., pp. 587-597, 1985.

3. Lowell, H. H., and N. Patton, "Response of Homogeneous and Two-Material Laminated Cylinders to Sinusoidal Environmental Temperature Change, with Applications to Hot Wire Anemometry and Thermocouple Psyometry," NACA TN 3514, September 1955.

4. Bulavin, P.E., and V.M. Kashcheev, "Solution of the Non-homogeneous Heat Conduction Equation for Multilayered bodies," International Chemical Engineering, vol. 5. No. 1, Jour. 1965, pp. 112-115.

5. Mulholland, G.P., "Diffusion through Laminated Orthotropic Cylinders," Fifth International Heat and Mass Transfer Conference, (Tokyo, Cu. 4.3, 1974.

6. Kerlin, T.W., et al., "Temperature Sensor Response Characterization," Electric Power Research Institute Report NP1486, August 1980.

7. Kannady, Roy, Jr., et al., "Martin Marietta Interactive Thermal Analysis System MITAS-II-NOS-FTN Version," Martin Marietta Data Systems, P.O. Box 179, Denver, Colorado 80201, April 1977.

8. Daryabeigi, K., R.L. Ash, and E.F. Germain, "Measurement of Connective Heat Transfer to Solid Cylinders Inside Ventilated Shrouds," AIAA-84-1725, 1984.

APPENDIX A

THERMOPHYSICAL PROPERTIES OF PRT's MATERIALS

Material	Thermal Conductivity $\frac{\text{Watt}}{\text{m } ^{o}\text{C}}$	Specific heat $\frac{\text{Watt Sec}}{\text{kg } ^{o}\text{C}}$	Density Kg/m^3
Platinum	71.6	132.725	21409.7 Kg/m^3
Aluminum Oxide	25.1	774.6	3943.6
Stainless Steel	27.69	502.428	7848.82

APPENDIX A

THERMOPHYSICAL PROPERTIES OF PRT's MATERIALS

Material	Thermal Conductivity $\frac{\text{Watt}}{\text{m } ^{o}\text{C}}$	Specific heat $\frac{\text{Watt Sec}}{\text{kg } ^{o}\text{C}}$	Density Kg/m^3
Platinum	71.6	132.725	21409.7 Kg/m^3
Aluminum Oxide	25.1	774.6	3943.6
Stainless Steel	27.69	502.428	7848.82

APPENDIX B

CONDUCTANCE FORMULAS FOR LAYERS HAVING LENGTH, L

Case 1. Homogeneous material with annular region:

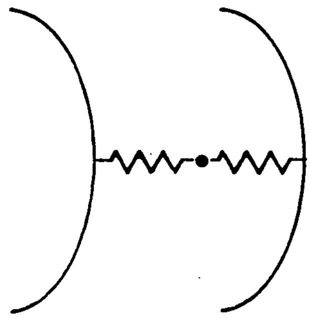

$$C = \frac{4 \Pi R L}{\ell n \left(r_{i+1}/r_i \right)}$$

Case 2. Annular region surrounded by another annular region with different thermal properties.

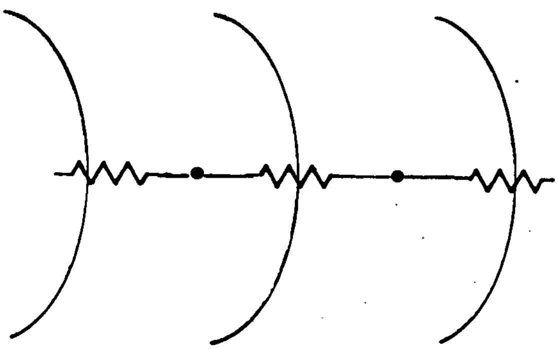

$$C = \frac{4 \Pi R_1 L}{\ell n \left(r_i/r_i \right)} + \frac{4 \Pi R_2 L}{\ell_n \left(r_{i+1}/r_i \right)}$$

Case 3. Innermost region with no heat transfer to any inner region ($T_{inner} = T_i$)

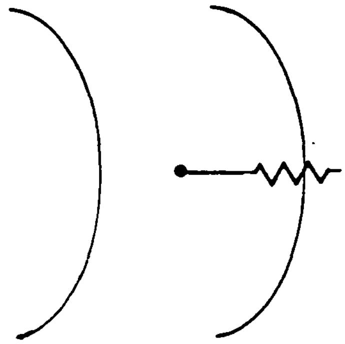

$$C = \frac{4 \Pi R L}{\ell n (r_i/r_{inner})}$$

Case 4. Annular region exposed to flowing fluid

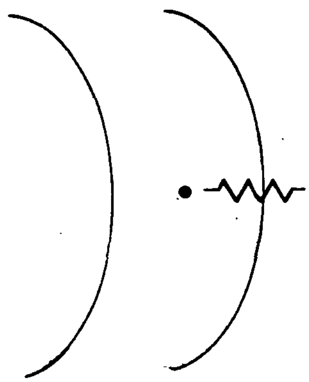

$$C = \frac{4 \Pi R L}{\ell n (r_o/r_i)} + 2 \Pi h r_o L$$

APPENDIX C

DATA FOR MITAS PROCEDURE FOR KERLIN'S HOLLOW CYLINDRICAL CASE

```
NOT RESTART
-EOR
     BCD 3TITLE DATA
     BCD 9KERLIN SOLID EXAMPLE
     BCD 9TRANSIENT ANALYSIS OF PRT
     END
 CC
     BCD 3NODE DATA
 CC

     9.88.0.-1.0
     10.88.0.1.0122E-3
     20.88.0.1.0122E-3
 C
     30.88.0.1.0122E-3
     40.88.0.1.0122E-3
     50.88.0.1.0122E-3
     60.88.0.1.0122E-3

CC
CC
     70.88.0.1.0122E-3
     80.88.0.1.0122E-3
     90.88.0.1.0122E-3
     -99.70.0.0.00
     END
C
```

```
C
      BCD 3CONDUCTOR DATA
      910.9.10.229925.564
      1020.10.20.11611.698
      2030.20.30.11763.753
      3040.30.40.11909.419
      4050.40.60.12067.946
      5060.50.60.12220.00
      6070.60.70.123172.056
      7080.70.80.12517.393
      8090.80.90.12676.248
      9099.90.99.136.710
      END
CC
      BCD 3CONSTANTS DATA
      ITEST=1
      TIMEO=00.0. TSTEPI=5.E-6.
      TIMEND=1.0E-4.TSTEPO=5.E-6.ITERMX=1500
      DRLXCA=0.00001. EXTLIM= 0.00
      NDSTOR=80. ARLXCA 0.00001
      END
C
```

```
BCD 3EXECUTION
FWDBCK
END
BCD 3OUTPUT CALLS
 TI= 88.0
 TF= 70.0
 ATIM = TIMEN * 3600.0
TH10= (TI-T10)/(TI-TF)
TH20= (TI-T20)/(TI-TF)
TH30= (TI-T30)/(TI-TF)
TH40= (TI-T40)/(TI-TF)
TH50= (TI-T50)/(TI-TF)
TH60= (TI=T60)/(TI-TF)
TH70= (TI=T70)/(TI-TF)
TH80= (TI-T80)/(TI-TF)
TH90= (TI-T90)/(TI-TF)
TPRINT
WRITE(NUSER1,20) ATIM,TH10,TH20,TH40,TH50,TH60,TH70,TH80,TH90
F 20 FORMAT(10(3X.F7.4)
     END
     BCD 3END OF DATA
```

APPENDIX D

DATA FOR MITAS PROCEDURE FOR ROSEMOUNT SENSOR

```
NOT RESTART
-EOR-
     BCD 3TITLE DATA
     BCD 9COMPARING WITH EXPERIMENTAL RESPONSE TIME
     BCD 9TRANSIENT ANALYSIS OF PRT
     END
CC
     BCD 3NODE DATA
CC
       9,32.0,-1.0
      10,32.0.144.37E-7
      20,32.0.1.1844
      30,32.0.1.1844
C
      -99,24.0.0.0
      END
C
C
      BCD 3CONDUCTOR DATA
      910,9,10,317207.97
      1020,10,20,106693.363
      2030,20,30,80631.824
      3099,30,99,4.000
      END
```

```
CC
      BCD 3CONSTANTS DATA
      ITEST=1
      TIMEO=00.0, TSTEPI=1.0
      TIMEND=40.0    .TSTEP
      DRLXCA= 0.0001    .EXTLIM= 0.00.ABSZRO=273.0
      NDSTOR=80. ARLXCA= 0.0001

      END
C
      BCD 3EXECUTION
      FWDBCK
      END
      BCD 3OUTPUT CALLS
       TI= 32.0
       TF= 24.0
       ATIM = TIMEN
      TH10=(TI-T10)/(TI-TF)
      TH20= (TI-T20)/(TI-TF)
      TH30= (TI-T30)/TI-TF)
      TPRINT
      WRITE(NUSER1.20) ATIM,TH10,TH30
F 20 FORMAT(4(3X.F7.4))
      END
      BCD 3END OF DATA
```